Synchrotron X-ray diffraction Studies of Ceramic Oxides

J. Bashir

Pakistan Institute of Nuclear Science & Technology
P.O. Nilore, Islamabad

Recent years have seen a dramatic growth in the applications of synchrotron powder diffraction measurements. Powder diffraction beam lines at synchrotron user facilities offer advantages of intensity, resolution and tunability, relative to conventional X-ray generators. SR powder diffraction has been used for a variety of experiments where high accuracy of data is important in crystal structure determination including both nuclear and magnetic crystal structure, space group resolution, charge distribution, and phase transformations.

…. Bit of History

- 1947 First synchrotron radiation seen
- 1961 First SR facility at NBS, Washington, USA
  - 180MeV
  - Measurement of Absorption Spectra of rare gases
- 1979 First experiment to assess the advantages of SR diffraction over conventional diffraction was carried out at Laboratory for High Energy Physics (KEK), Japan.

By 1983, foundations of SR powder diffraction were well laid out. Since that time the techniques employing SR are now having a major impact on several areas of physics, chemistry and biological sciences. It has now become possible to perform entirely new type of experiments, for example, high temperature, high pressure, magnetic scattering and kinetic or time – resolved crystallography.

Characteristics of Radiation

	Electrons			X-Rays			Hard X-rays		Neutrons		
Energy	100keV	200keV	500keV	Fe 7keV	Cu9keV	Mo 20keV	35keV	80keV	1 meV	10 meV	100 meV
Wavelength (nm)	0.0037	0.0025	0.0014	0.194	0.154	0.071	0.035	0.015	0.9	0.29	0.09
Velocity (m/s)	$1.7x10^8$	$2.1x10^8$	$2.6x10^8$	$3x10^8$	$3x10^8$	$3x10^8$	$3x10^8$	$3x10^8$	430	1400	3100
Temperature (K)	$1x10^9$	$2x10^9$	$5x10^9$	$0.8x10^8$	$1x10^8$	$2x10^8$	$3.5x10^8$	$8x10^8$	12	116	580
Penetration in Fe	~100nm			~10µm			1mm-1cm		~ 5 cm		

Synchrotron Techniques

Main techniques

- Absorption based: characteristic absorption of X-rays by samples, especially in the region of absorption edges used to deduce local structure
- Attenuation/absorption used in radiography/tomography
- Diffraction uses a monochromatic beam for structure determination, stress, phase identification, etc

The diverse uses of synchrotrons

- Medical imaging and therapy
- Environment
- Forensics
- Manufacturing
- Medicine and pharmaceuticals
- Agriculture
- Minerals
- Micromachining
- Materials sciences and engineering

Oxide based materials

- The majority of advanced materials used in magnetic, conductivity, superconductivity, ferroelectric, catalytic and battery applications are solid metal oxides. Metal oxide chemistry is dominated by classes of materials having crystal structures derived from simpler parent structures such as perovskite or rutile.
- Small lattice distortions, which are critical to the key electronic and physical properties of these oxides, usually lead to lower symmetries and superstructures. These distortions are characterised by subtle peak splittings and the appearance of weak superlattice reflections in diffraction data.
- The detection and understanding of such distortions requires the high resolution afforded by synchrotron radiation

Science

The impact of powder diffraction and the use of the Rietveld method for structural crystallography is

MASSIVE

In the last decade, powder diffraction has been the technique of choice to provide vital structural insight in diverse areas:

Science

- **High Temperature Cuprate and other Oxide Superconductors:**
  - Structure and crystal-chemistry of the high-Tc superconductor $YBa_2Cu_3O_{7-x}$, ***Nature***, **327**, 310-312 (1987)
  - Superconductivity near 30-K without copper - the $Ba_{0.6}K_{0.4}BiO_3$ Perovskite, ***Nature***, **332**, 814-816 (1988)
  - Synthesis and superconducting properties of the strontium copper oxy-fluoride $Sr_2CuO_2F_{2+d}$, ***Nature***, **369**, 382(1994)
  - Cation effects in doped La_2CuO_4 superconductors, ***Nature***, **394**, 157-159 (1998)
  - Systematic cation disorder effects in $L_{1.85}M_{0.15}CuO_4$ superconductors, ***Phys. Rev. Lett***., **83**, 3289-3292 (1999)
- **MgB_2 and Borocarbide Superconductors:**
  - Structure of the 13-K superconductor $La_3Ni_2B_2N_3$ and the related phase LaNiBN", ***Nature***, **372**, 759-761 (1994)
  - MgB_2 superconducting thin films with a transition temperature of 39 Kelvin", ***Science***, **292**, 1521-1523 (2001)
  - Superconductivity at 39 K in magnesium diboride", ***Nature***, **410**, 63(2001)

Science

- **C_{60} and its Superconducting Derivatives:**
  - Superconductivity at 28 K in Rb_xC_{60}, ***Phys. Rev. Lett.*, 66**, 2830(1991)
  - Intercalation of ammonia into K_3C_{60}, ***Nature***, **364**, 425-427 (1993)
  - Crystal-structure, bonding, and phase-transition of the superconducting Na_2CsC_{60} Fulleride, ***Science***, **263**, 950-954 (1994)
  - Structural and electronic properties of the noncubic superconducting fullerides A ' C-4(60) (A '= Ba, Sr), ***Phys. Rev. Lett***., **83**, 2258(1999)
- **Cathode and Electrolytic Materials for Portable, Rechargable Batteries:**
  - Crystal-structure of the polymer electrolyte poly(ethylene Oxide)$_3$:$LiCF_3SO_3$, ***Science***, **262**, 883-885 (1993)
  - Synthesis of layered $LiMnO_2$ as an electrode for rechargeable lithium batteries, ***Nature***, **381**, 499-500 (1996)
  - Structure of the polymer electrolyte poly(ethylene oxide)$_6$:$LiAsF_6$, ***Nature***, **398**, 792-794 (1999)
  - Ionic conductivity in crystalline polymer electrolytes, ***Nature***, **412**, (2001)

Science

- **Giant Magneto-Resistive Materials**
  - Simultaneous Structural, Magnetic, and Electronic-Transitions in $La_{1-x}Ca_xMnO_3$ with x=0.25 and 0.50, ***Phys. Rev. Lett***., **75**, 4488-4491 (1995)
  - Colossal magnetoresistance without Mn^{3+}/Mn^{4+} double exchange in the stoichiometric pyrochlore $Tl_2Mn_2O_7$, ***Science***, **273**, 81-84 (1996)
  - Lattice effects and magnetic order in the canted ferromagnetic insulator $La_{0.875}Sr_{0.125}MnO_{3+d}$", ***Phys. Rev. Lett***., **76**, 3826-3829 (1996)
  - Direct observation of lattice polaron formation in the local structure of $La_{1-x}Ca_x MnO_3$ ", ***Phys. Rev. Lett.,*** **77**, 715-718 (1996)
  - Colossal magnetoresistance in Cr-based chalcogenide spinels", ***Nature***, **386**, 156-159 (1997)
  - Electrostatically driven charge-ordering in Fe_2OBO_3, ***Nature***, **396**, 655-658 (1998)
  - Optimal T-C in layered manganites: Different roles of coherent and incoherent lattice distortions, ***Phys. Rev. Lett***., **83**, 1223-1226 (1999)
  - Formation of isomorphic Ir^{3+} and Ir^{4+} octamer and spin dimerisation in the spinel $CuIr_2S_4$, ***Nature***, **416** 155-158 (2002)

Science

- **First Metal Oxide Hydride:**
  - The hydride anion in an extended transition metal oxide array: $LaSrCoO_3H_{0.7}$, ***Science***, **295**, 1882 (2002)
- **New Dielectric Materials:**
  - Enhancement of the dielectric-constant of Ta_2O_5 through substitution with TiO_2, ***Nature***, **377**, 215-217 (1995)
- **Highly-Reactive Molecular Species:**
  - Crystal and molecular-structures of rhenium heptafluoride, ***Science***, **263**, 1265-1267 (1994)
- **Magnetic Nanomaterials:**
  - Monodisperse FePt nanoparticles and ferromagnetic FePt nanocrystal superlattices, ***Science***, **287**, 1989-1992 (2000)
  - Size-dependent grain-growth kinetics observed in nanocrystalline Fe", ***Phys. Rev. Lett.*, 86**, 842-845 (2001)

Fig.1

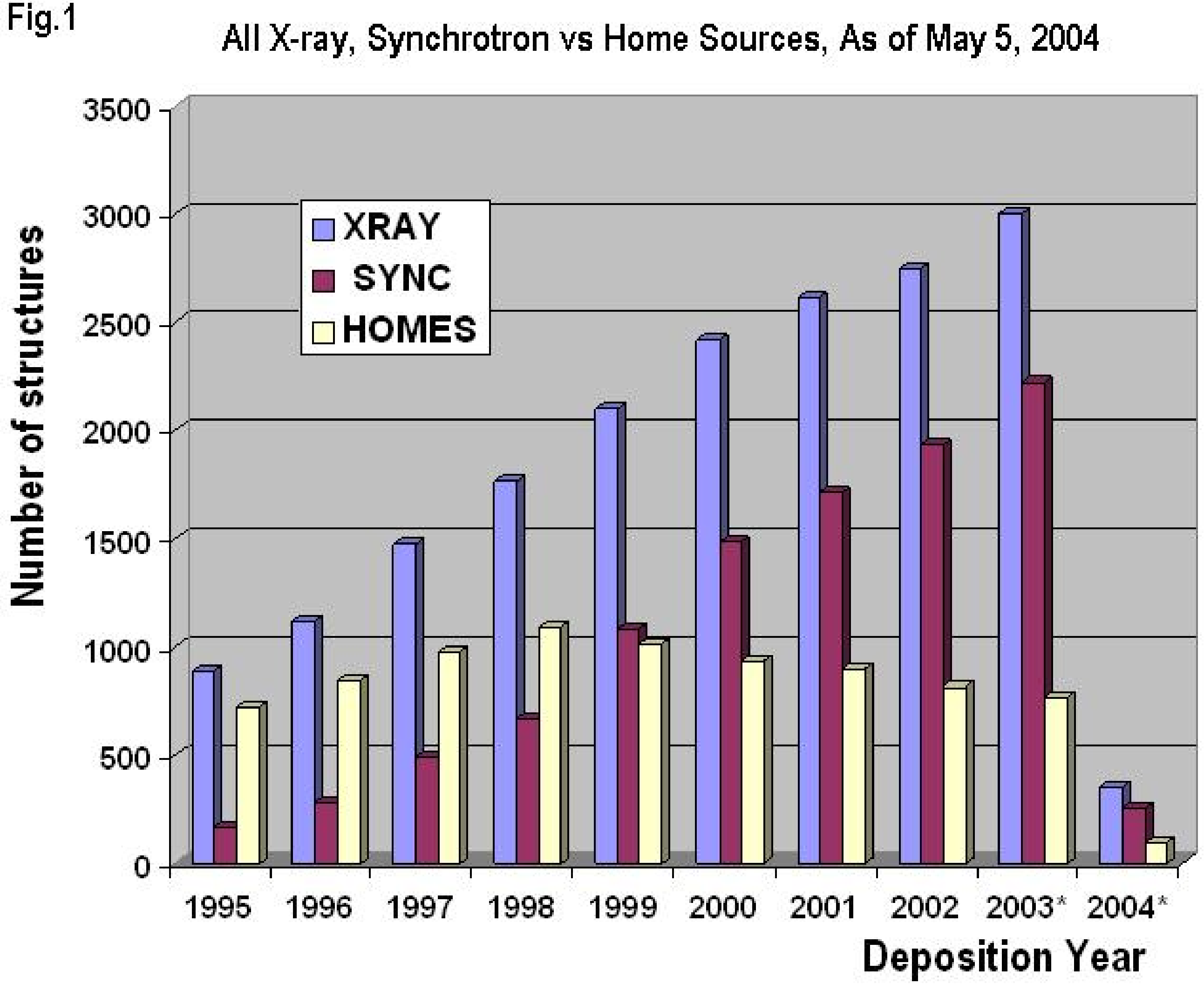
All X-ray, Synchrotron vs Home Sources, As of May 5, 2004
Number of structures
3500
3000
2500
2000
1500
1000
500
0
XRAY
SYNC
HOMES
1995
1996
1997
1998
1999
2000
2001
2002
2003*
2004*
Deposition Year

Properties of synchrotron light

- **High brightness:** synchrotron light is extremely intense (10^{12} times more intense than that from conventional x-ray tubes) and and are highly collimated.
- **Wide energy spectrum:** synchrotron light is emitted with energies ranging from infrared light to hard, energetic (short wavelength) x-rays.
- **Tunable**: through sophisticated monochromators and insertion devices it is possible to obtain an intense beam of any selected wavelength.

Higher Flux

  - Smaller Samples (milligram)
  - Collect more data in a shorter amount of time
  - Collect better quality data (increased resolution)
- Tunable energy
  - Spectrum of x-ray energies available for specialized experiments

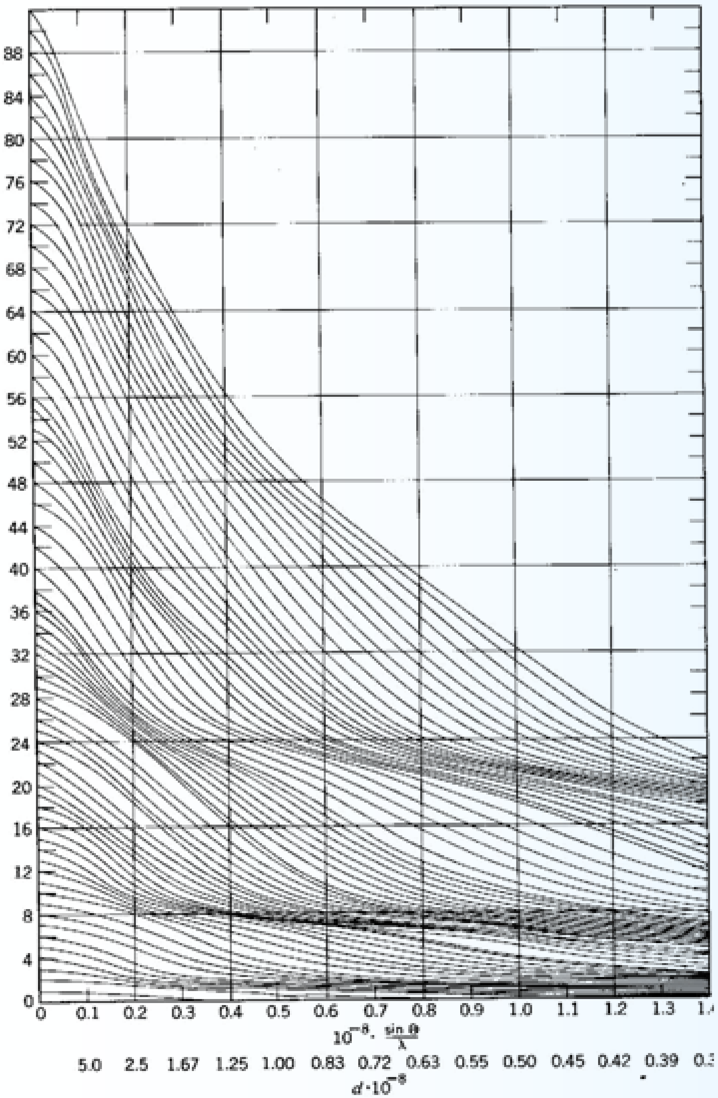

88
84
80
76
72
68
64
60
56
52
48
44
40
36
32
28
24
20
16
12
8
4
0
0 0.1 0.2 0.3 0.4 0.5 0.6 0.7 0.8 0.9 1.0 1.1 1.2 1.3
10^-8 · sin θ / λ
5.0 2.5 1.67 1.25 1.00 0.83 0.72 0.63 0.55 0.50 0.45 0.42 0.39
d·10^-8

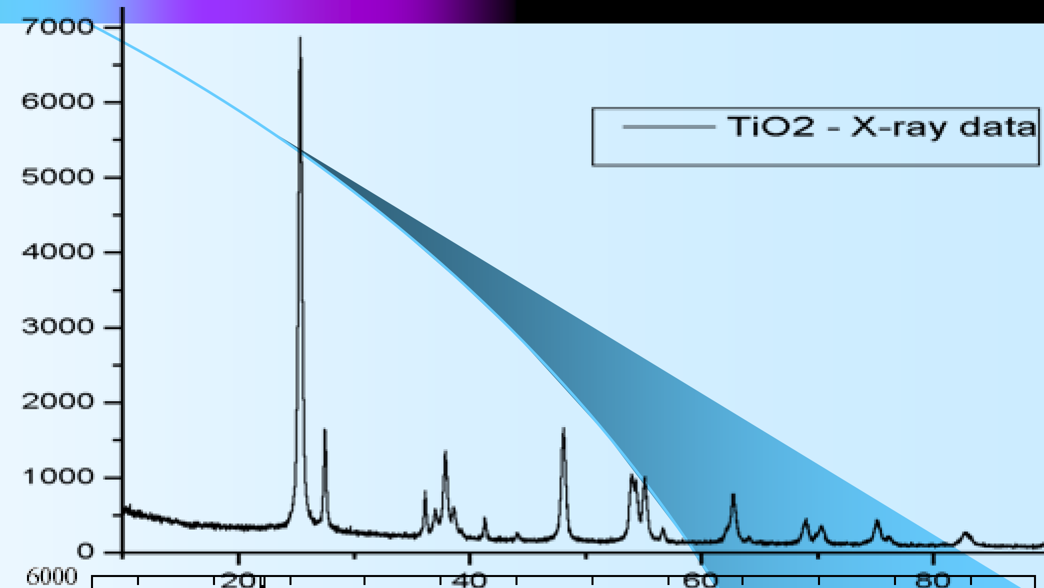

TiO2 - X-ray data
7000
6000
5000
4000
3000
2000
1000
0
20
40
60
80

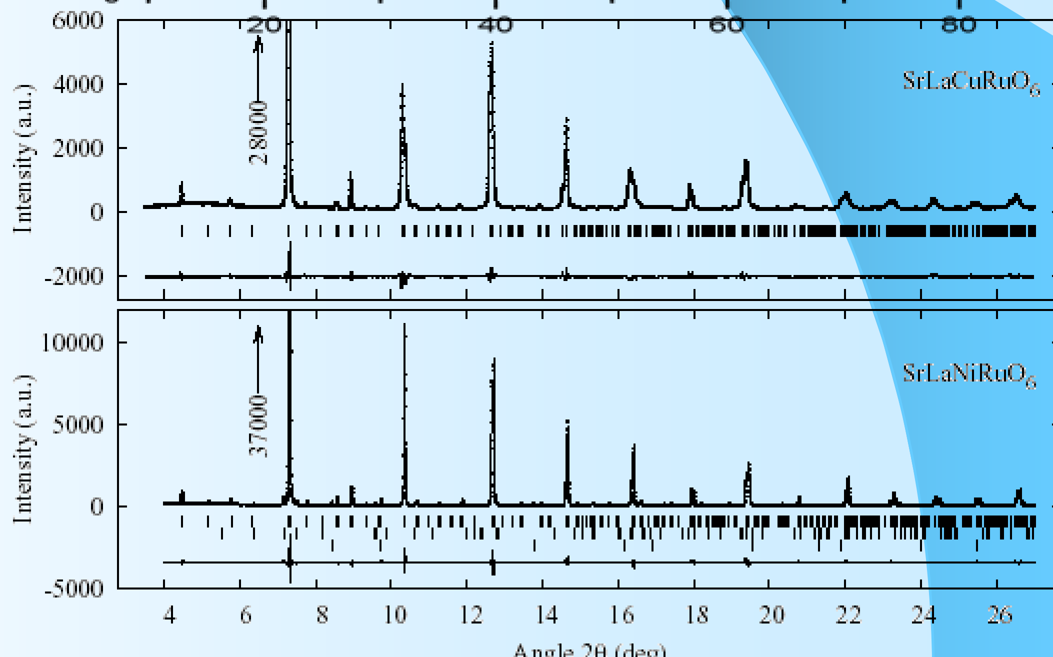

SrLaCuRuO6
28000
Intensity (a.u.)
6000
4000
2000
0
-2000
SrLaNiRuO6
37000
Intensity (a.u.)
10000
5000
0
-5000
4 6 8 10 12 14 16 18 20 22 24 26
Angle 2θ (deg)

Relative Scattering Powers of the Elements

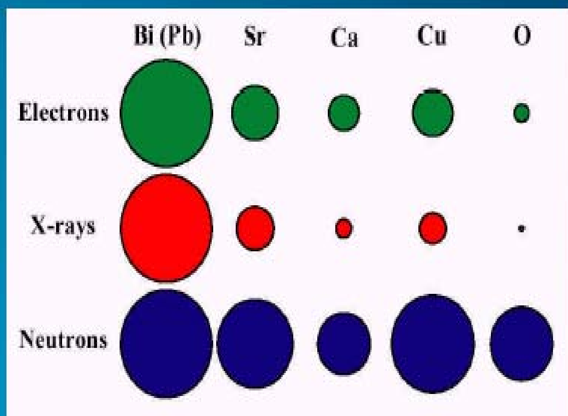

Neutrons scatter strongly from light elements

(Because neutron scattering is a nuclear interaction)

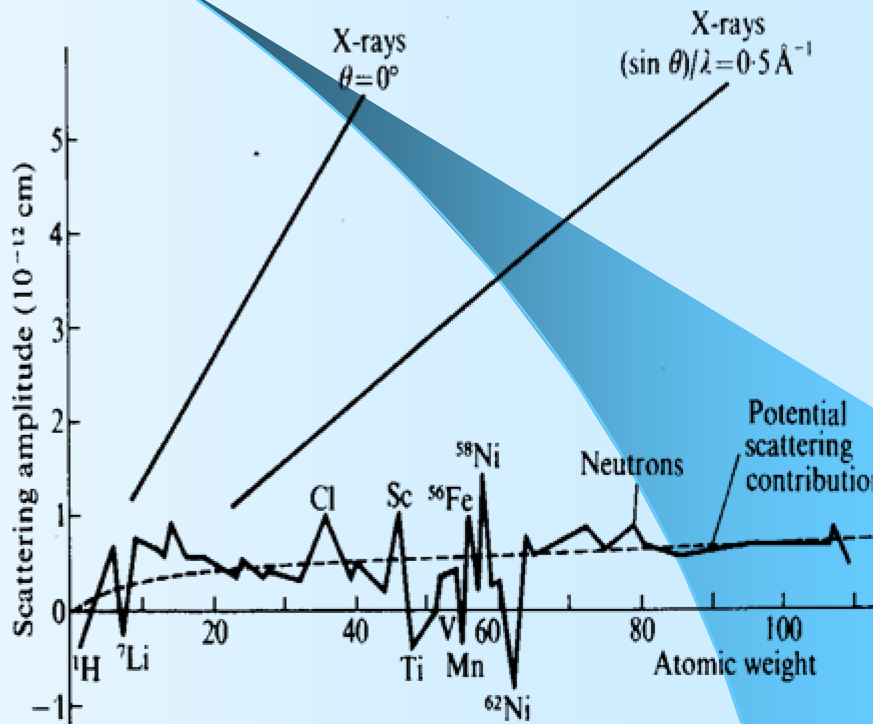

Rietveld Refinement

What we start with

- Space Group
- Unit Cell parameters
- Atomic Positions
- Atomic Occupancies

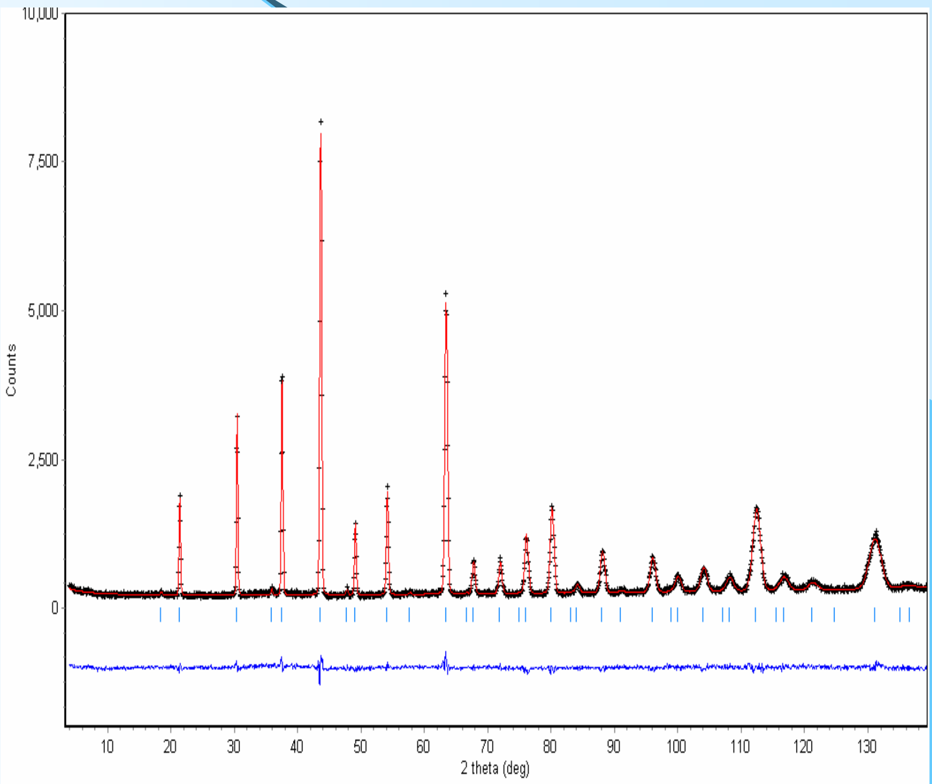

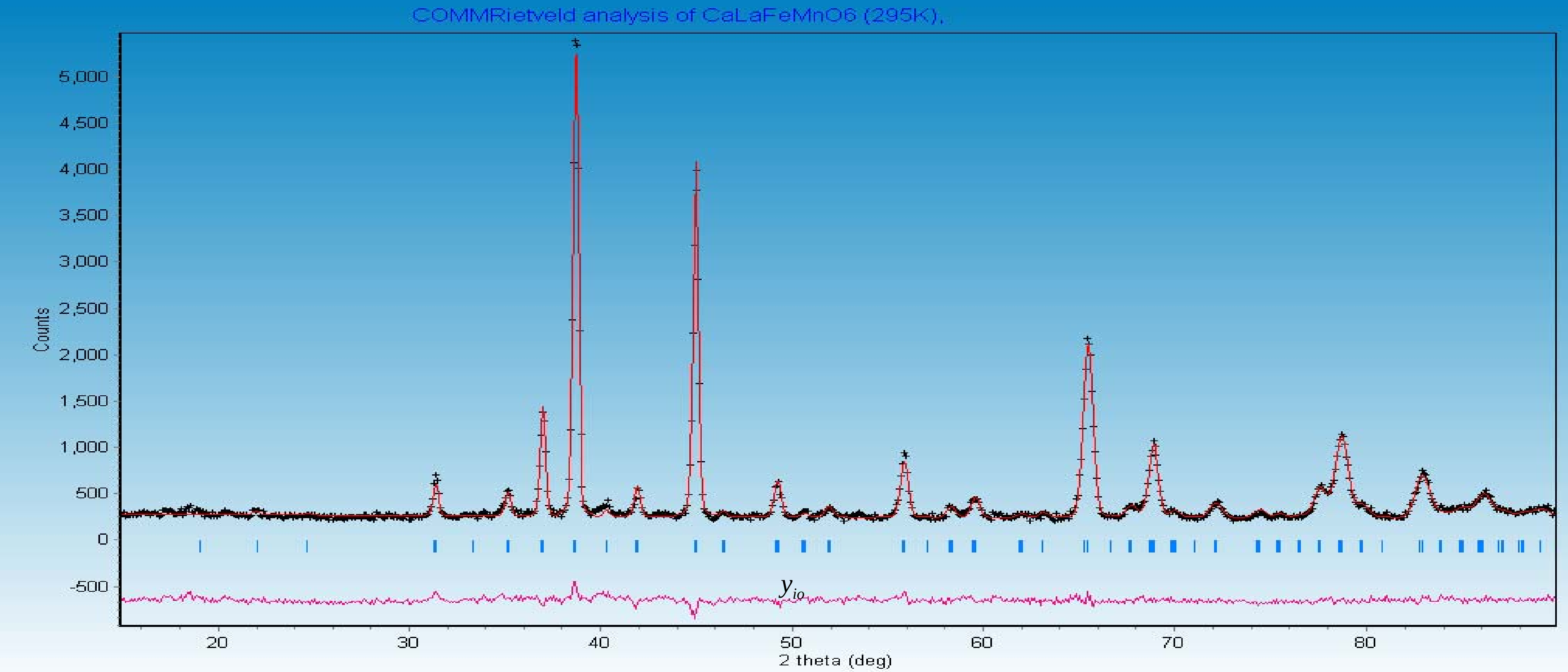

The basis of the Rietveld method is the equation $y_{ic} = y_{ib} + \sum_p \sum_k G_{ik}^p I_k$

where y_{ic} the net intensity calculated at point i in the pattern, y_{ib} is the background intensity, G_{ik} is a normalised peak profile function, and $I_k = Sm_k L_k |F_k|^2 P_k A_k E_k$ is the intensity of the k^{th} Bragg reflection.

$$R_p = \sum |y_{ic} - y_{io}| \Big/ \sum y_{io} \qquad R_p = \left[\sum w_i (y_{io} - y_{ic})^2 \Big/ \sum w_i y_{io}^2 \right]^{1/2}$$

Examples

1. La_2NiRuO_6
2. $ALaMnBO_6$ (A = Ca, Sr, Ba & B = Mn, Ru)

La_2NiRuO_6

- **Galasso and Darby* reported the La_2NiRuO_6 to be cubic [a = 7.90 Å Space group = Fm3m]**
- **Cubic with $P4_232$ space group.**

* F.S. Galasso, *Structure, Properties and Preparation of perovskite-type compounds*.

Pergamon Press Inc. 1969

Fernandez, *et al J. Sol. State Chem. 32 (1980) 97–104.*

La_2NiRuO_6 – Neutron Diffraction

Space group Pbnm, a = 5.5675(1)Å, b = 5.5952(1)Å, c = 7.8734(2)Å

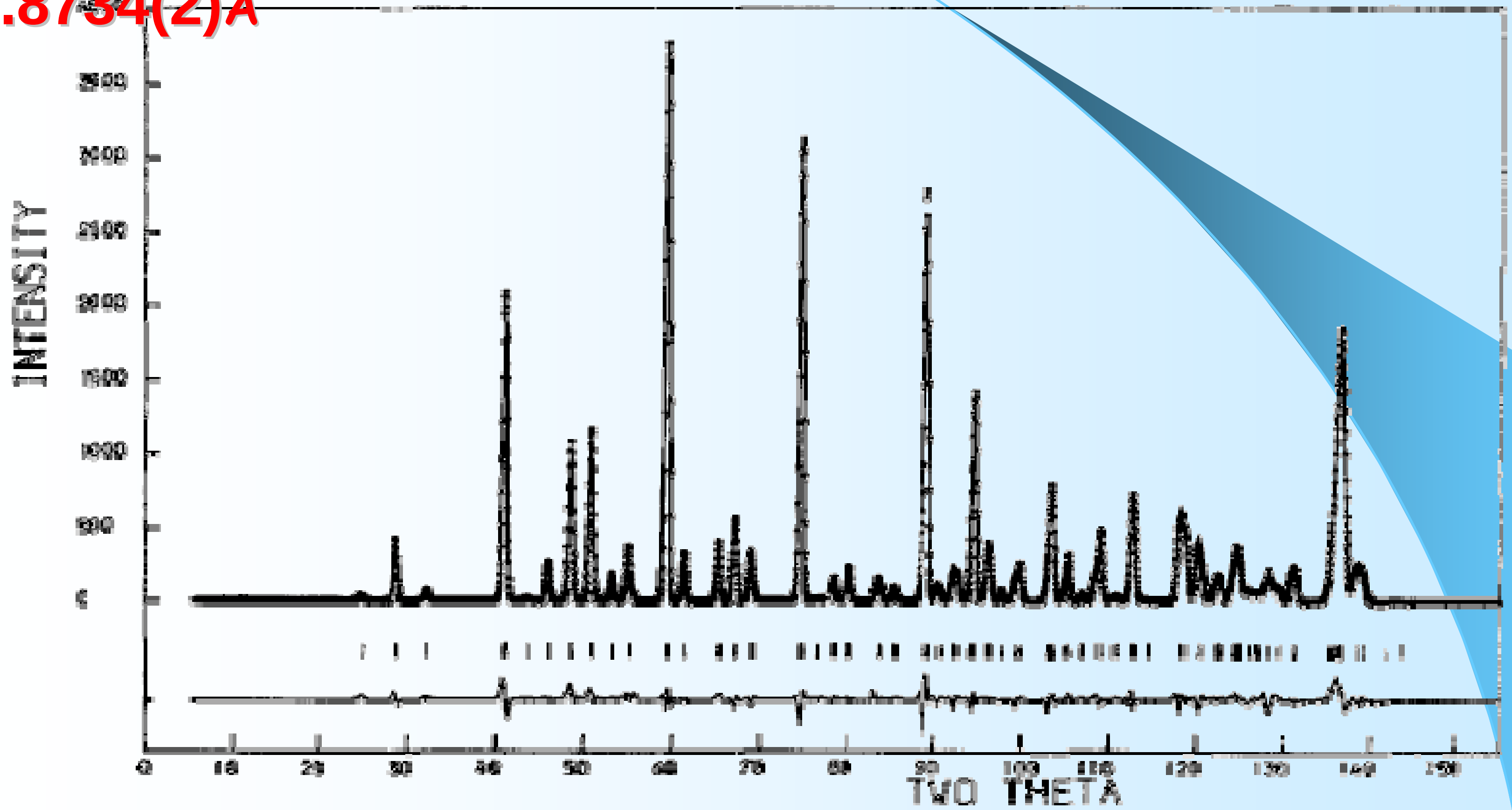

Reference: Battle & Jones, Mat. Res. Bull.,22(1987)1623

La_2NiRuO_6 – Neutron Diffraction

Monoclinic, $P2_1/n$.

a = 5.5688(4)Å, b = 5.5984(4)Å, c = 7.8764(6) Å, β = 90.18(I) °

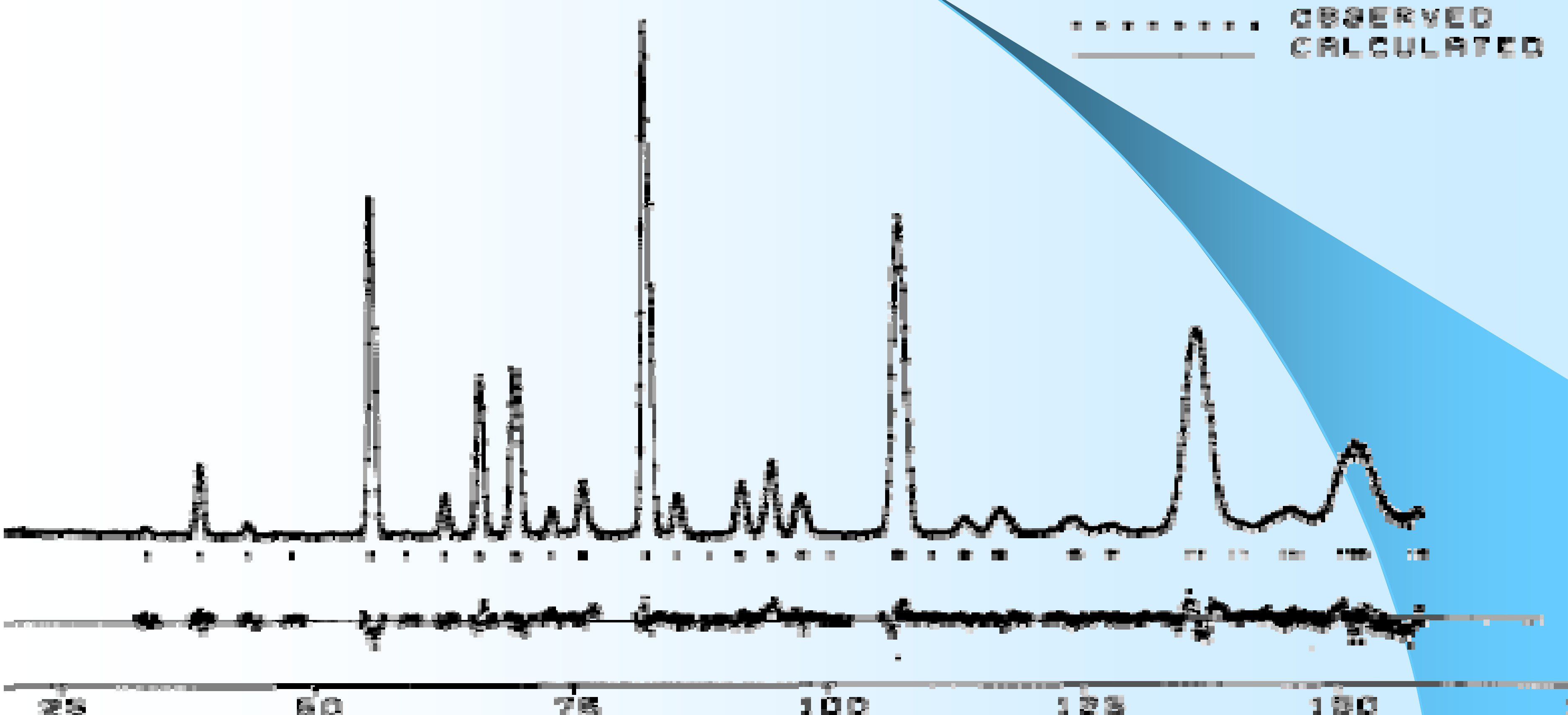

Reference: Seinen et al, Mat. Res. Bull.,22(1987)535.

La_2NiRuO_6 – Synchrotron X-ray Diffraction

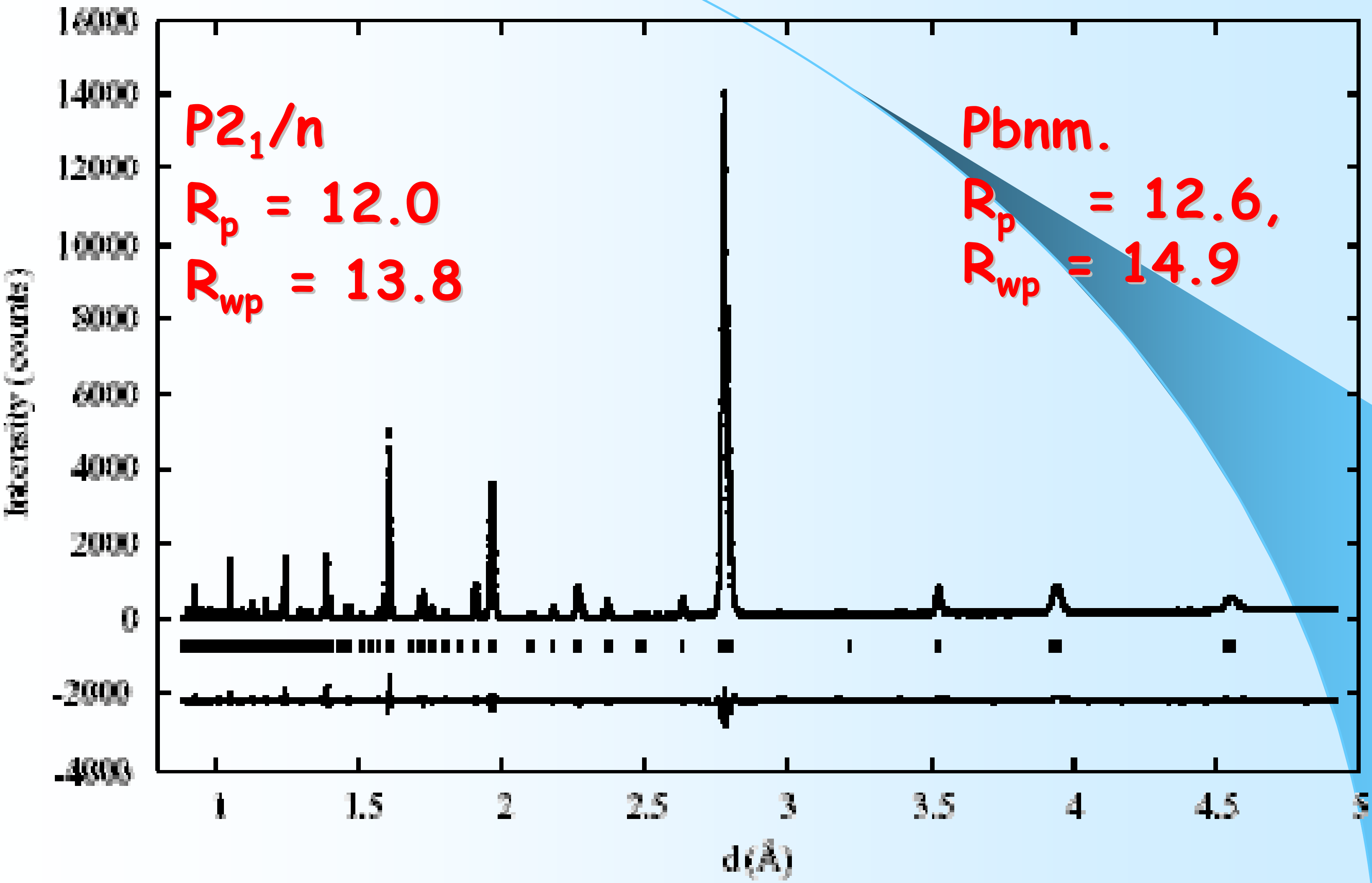

Reference : M. Gateshki et al, Materials Research Bulletin 38 (2003) 1661–1668

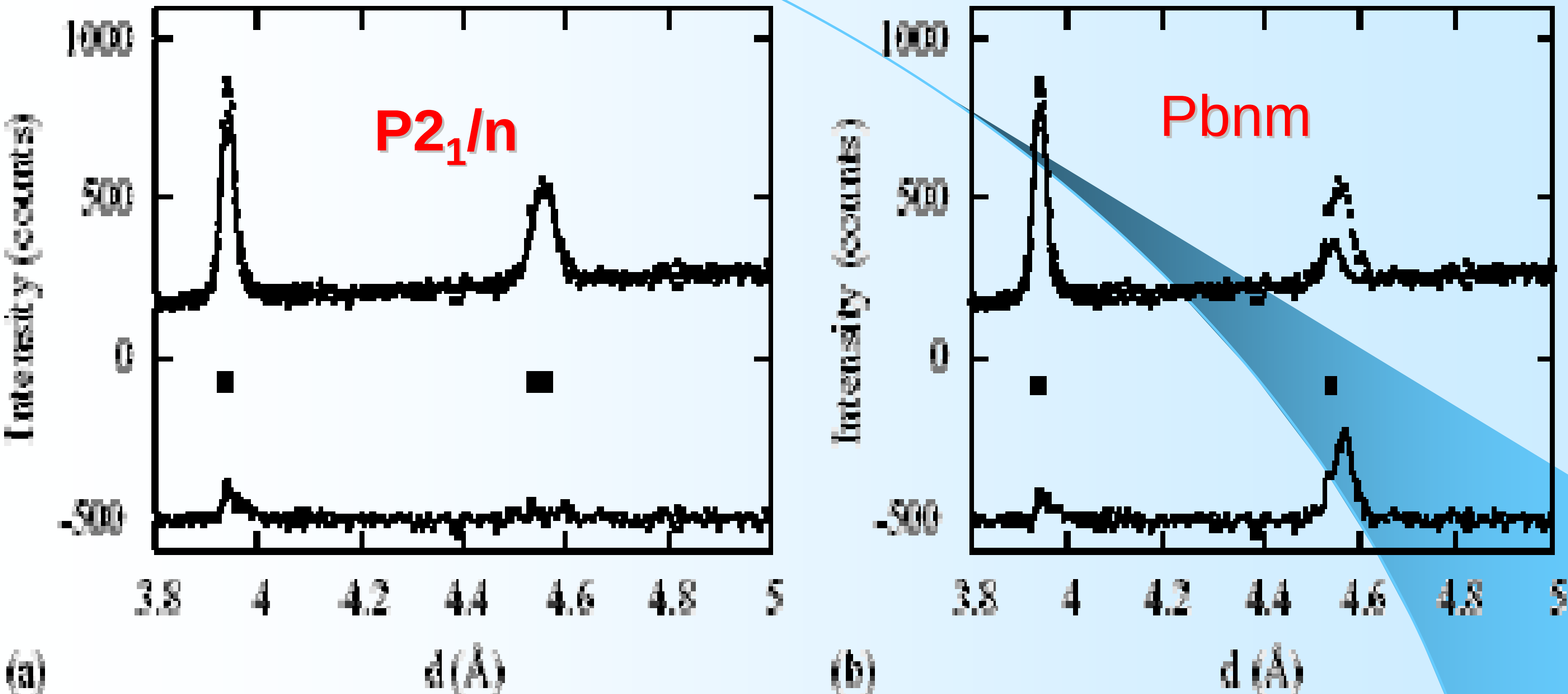

A section of the **laboratory X-ray** diffraction pattern refined with the P2$_1$/n (a) and Pbnm (b) space groups. The structural model with P2$_1$/n space group fits better the experimental data. The Bragg positions calculated for both, Kα_1 and Kα_2, are shown.

Reference : M. Gateshki et al, Materials Research Bulletin 38 (2003) 1661–1668

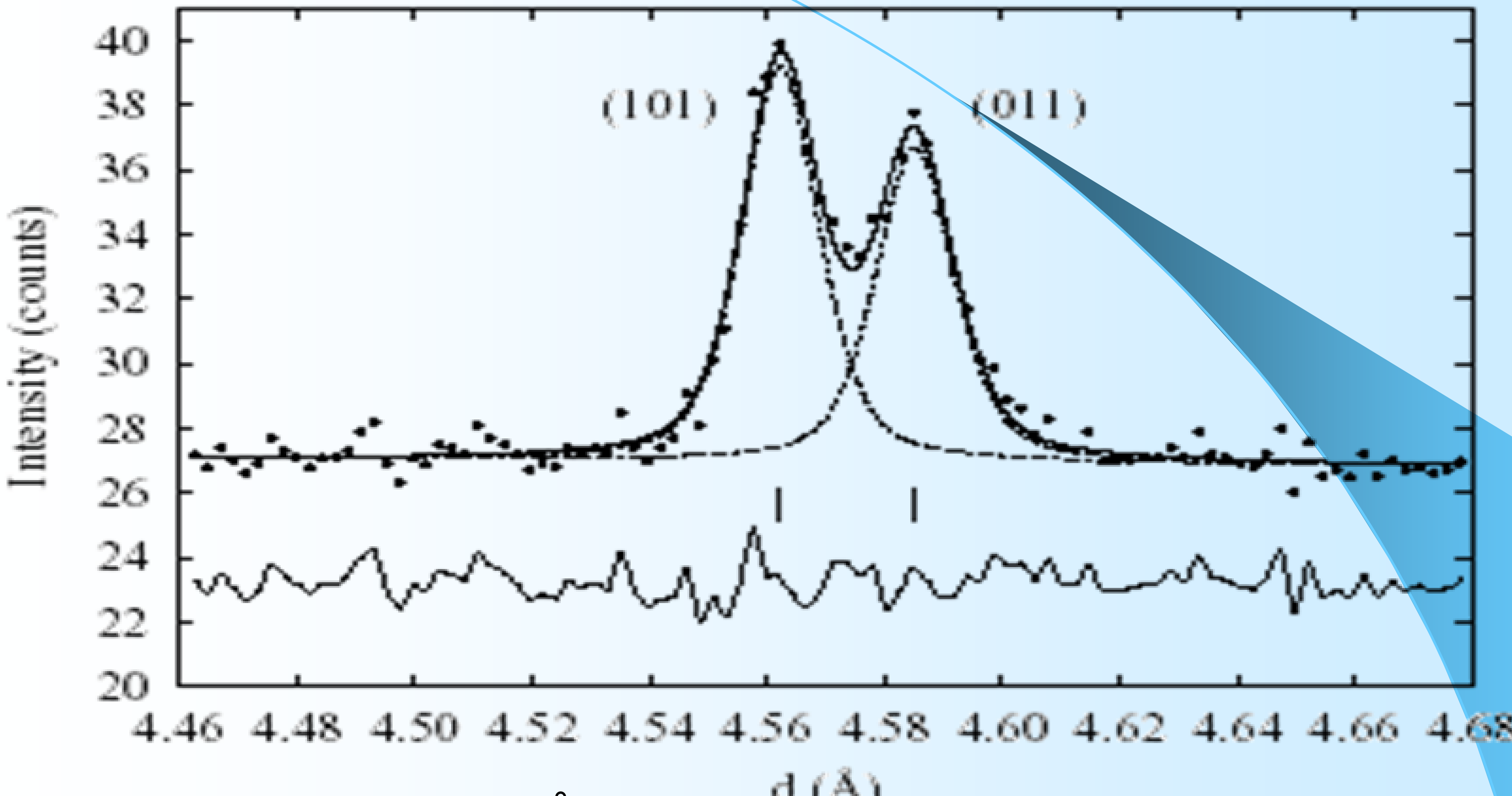

Synchrotron radiation (λ = 0.8 Å) diffraction data from a short 2θ range around d = 4:56 Å. Lines represent the profile fit obtained with a two-peak model. Data indexed with $P2_1/n$ space group. The presence of the (0 1 1) reflection in the diffraction pattern confirms the ordered arrangement of the B-cations in La_2NiRuO_6

Reference : M. Gateshki et al, Materials Research Bulletin 38 (2003) 1661–1668

$CaLaMnFeO_6$ - Synthesis

Starting Materials: $CaCO_3$, La_2O_3, MnO_2, Fe_2O_3

- CALCINATION: 1000 C FOR 18 HOURS IN AIR
  1100 C FOR 18 HOURS IN AIR
  1200 C FOR 18 HOURS IN AIR
- PELLETIZATION: 12mm DIAMETER & 2mm THICK PELLETS
- SINTERING: 1250 C FOR 72 HOURS IN AIR
- ANNEALING: 900 C FOR 48 HOURS IN O_2
- COOLING: FURNACE COOLED

$CaLaMnFeO_6$ - Fm3m

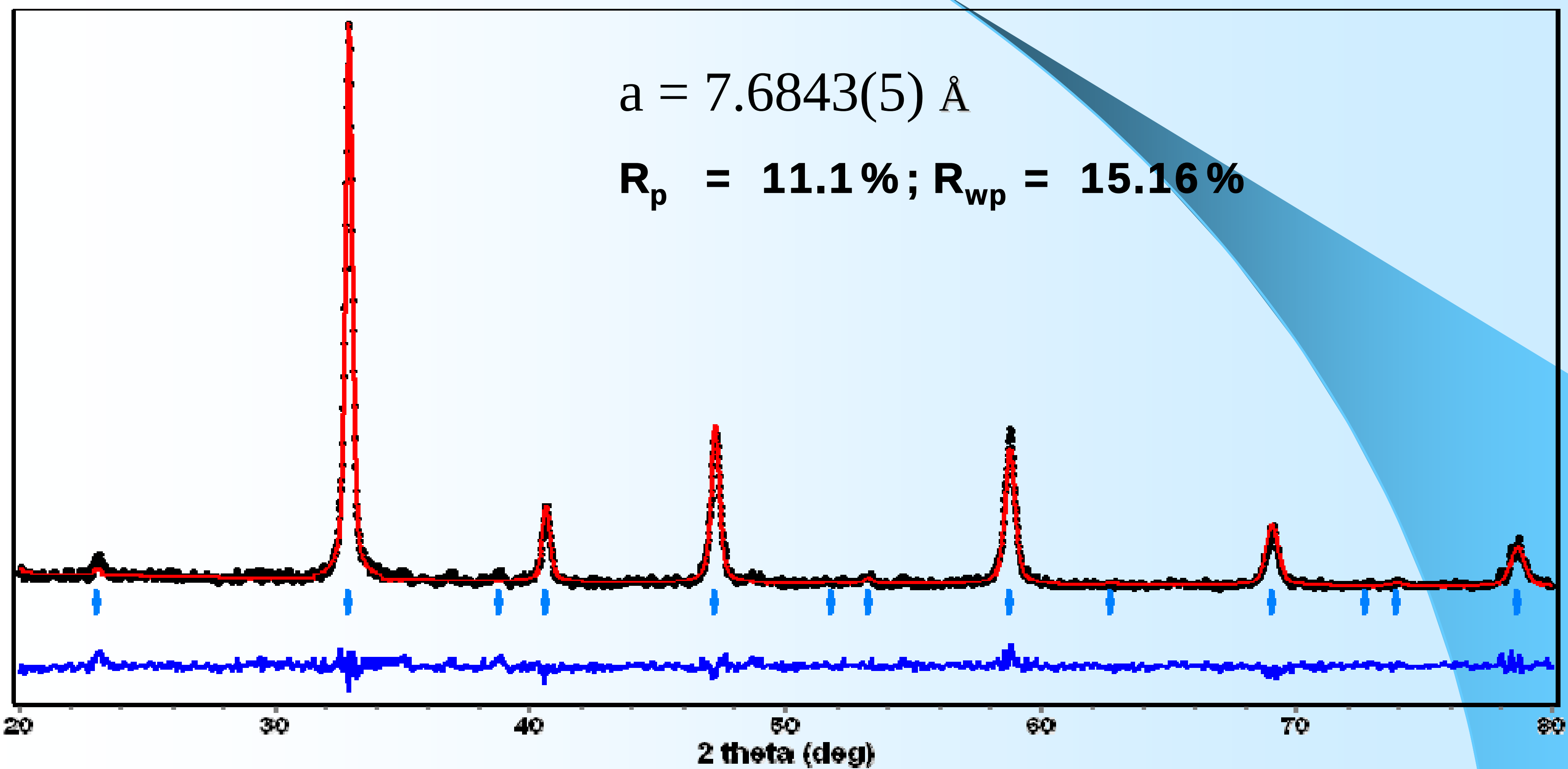

The observed (+) and calculated X-ray diffraction pattern of $CaLaMnFeO_6$ refined in space group Fm3m. Arrows indicate the weak unindexed reflections.

$CaLaMnFeO_6$

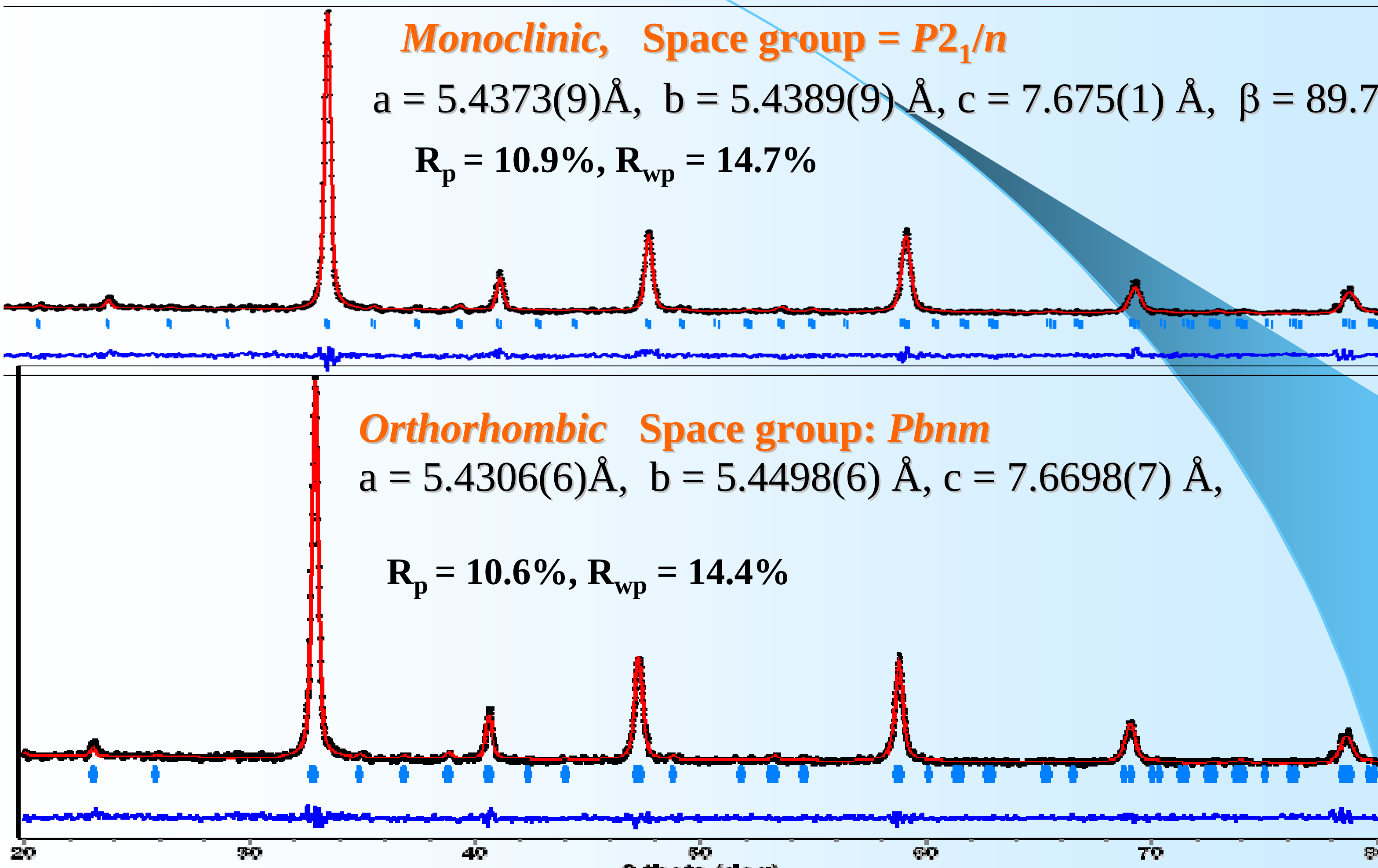

Fig. The X-ray diffraction pattern can be fitted in space group $P2_1/n$ (top) and Pbnm(bottom). Since the R-factors are comparable, it is not possible from laboratory X-ray diffraction measurements to assign the correct space group.

$SrLaMnFeO_6$

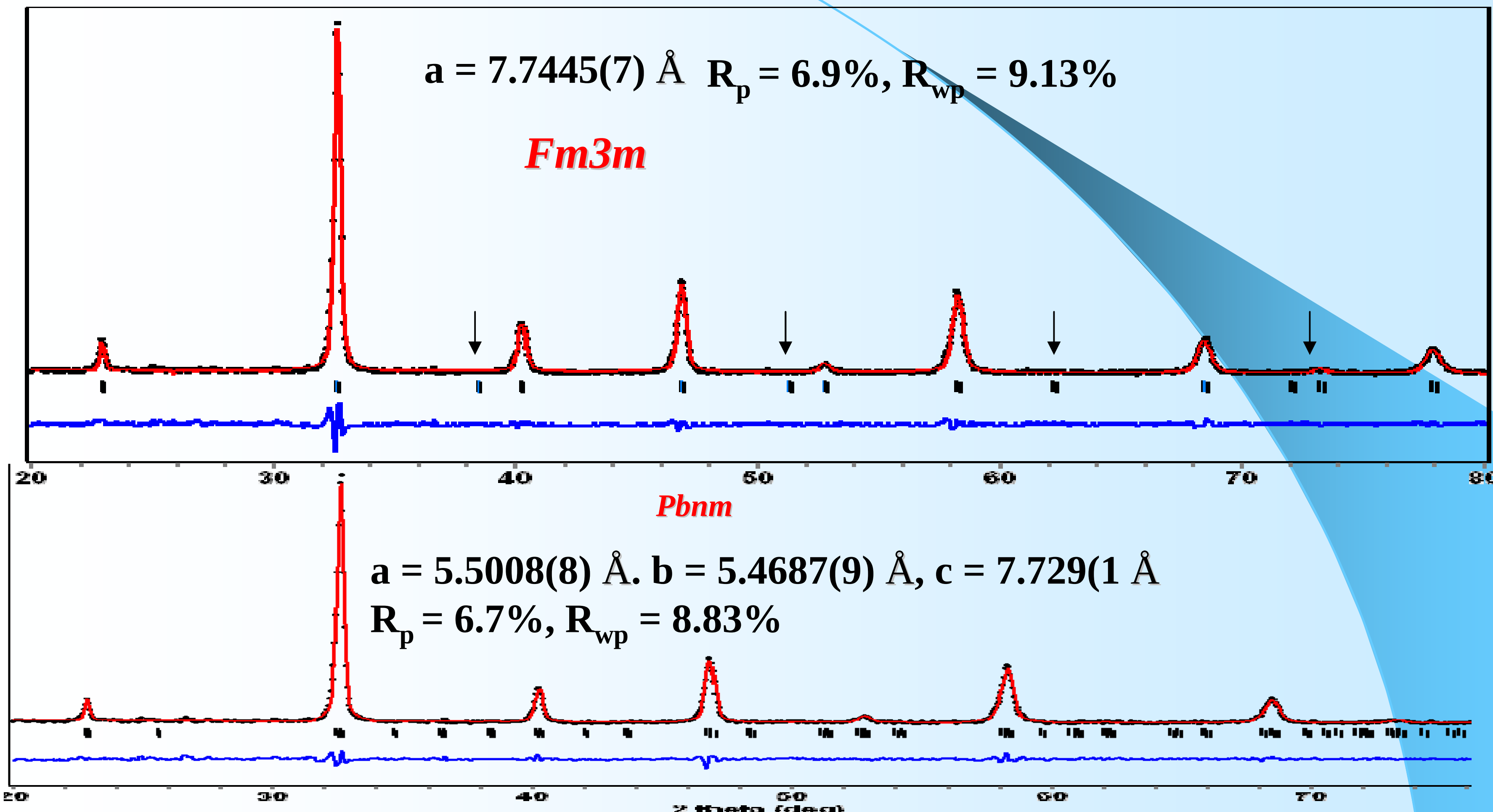

Refinement of X-ray diffraction data of $SrLaMnFeO_6$ in space group Fm3m (Top) and Pbnm (bottom). Arrows indicate unidexed reflections.

What is the Crystal Structure of ALaMnFeO6 ?

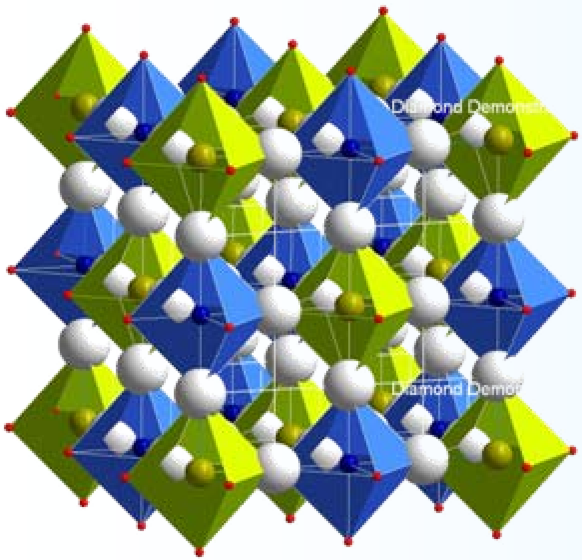

Cubic
Fm3m

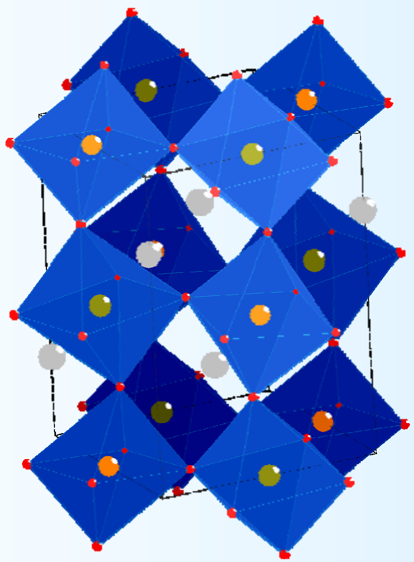

Monoclinic
$P2_1/n$

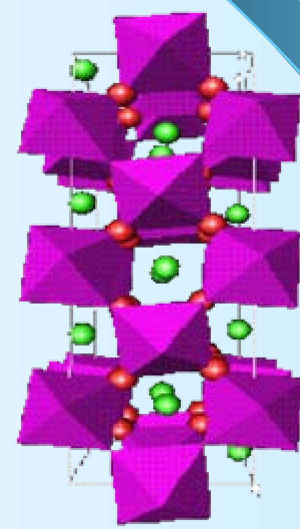

Orthorhombic
Pbnm

ICTP-ELETTRA Users Programme

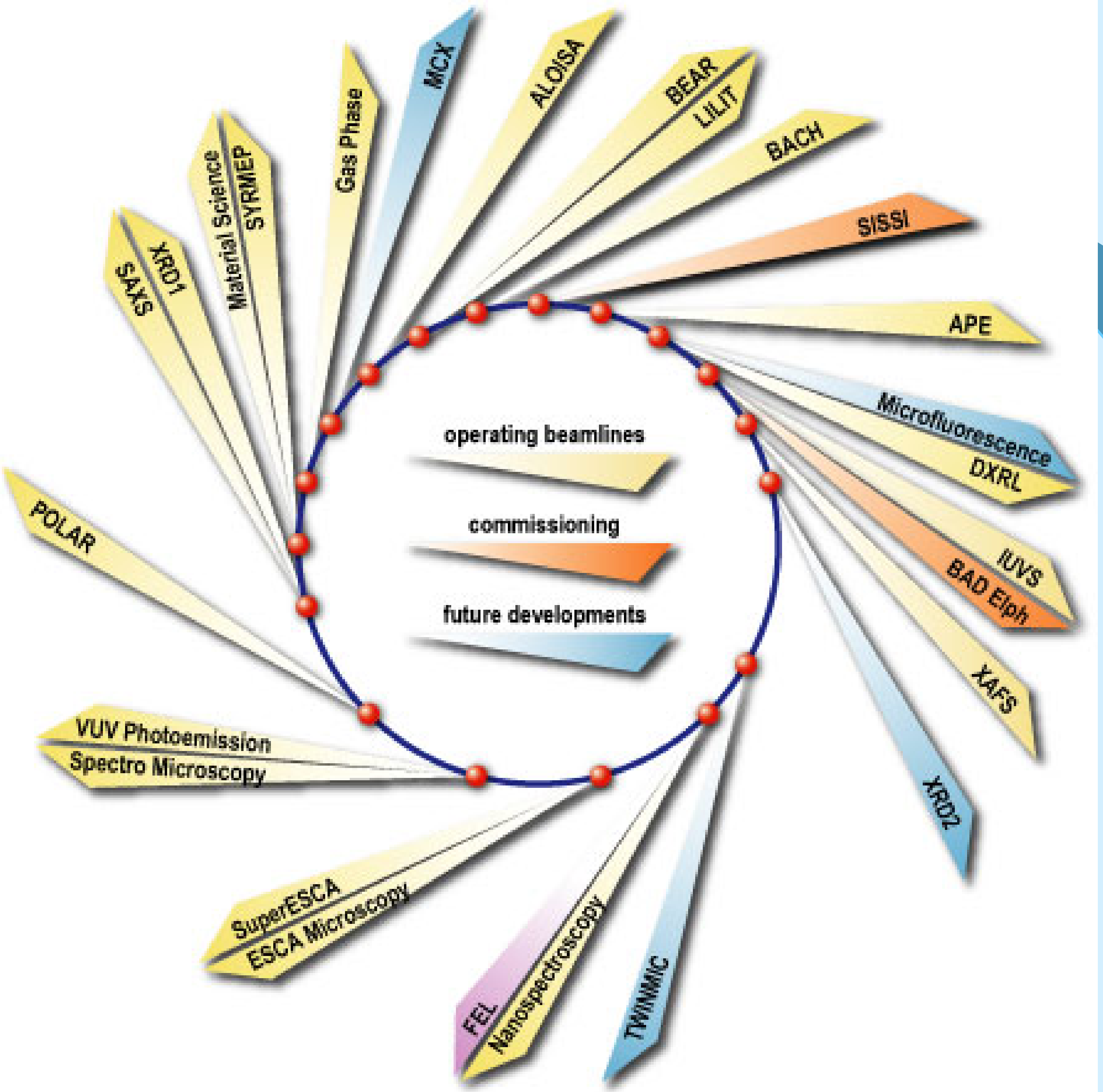

ICTP-ELETTRA Users Programme

- The ICTP-ELETTRA Users Programme is offering access to the synchrotron radiation facility ELETTRA in Trieste in the years 2002-2006 to scientists who are citizens of developing countries and work in those countries. Up to an annual total of 1500 hours can be made available within this programme for beamtime applications at any of the existing ELETTRA beamlines.
- The programme is offering a limited number of grants to cover travel and living expenses of individuals and small groups who are meant to participate in the beamtime at ELETTRA. The number of scientists who can receive support depends on the number of allocated shifts and available funds:

ICTP-ELETTRA Users Programme

In order to participate in the ICTP-ELETTRA Users Programme it is necessary to:

Submit an application for beam time following the usual ELETTRA procedure;

There are two deadlines every year:

- **February 28th**: for proposals eligible for the user period starting from July 1st to December 31st;
- **August 31st**: for proposals eligible for the user period starting from January 1st to June 30th.

The proposed experiments will be selected for beam time assignment on the basis of their scientific merit..